Journal of Sound and Vibration (2000) **237**(1), 145–161
doi:10.1006/jsvi.2000.3054, available online at http://www.idealibrary.com on IDEAL®

SPATIAL TRUNCATION IN MODELS OF NON-LINEAR VIBRATING SYSTEMS

D. E. Adams

Purdue University, School of Mechanical Engineering, Ray W. Herrick Laboratories, West Lafayette, IN 47907-1077, *U.S.A.*

AND

R. Allemang, A. W. Phillips and R. H. Wynn Jr

University of Cincinnati, Structural Dynamics Research Laboratory, PO Box 210072, *Cincinnati, OH* 45221-0072, *U.S.A.*

(*Received* 20 *October* 1999, *and in final form* 13 *April* 2000)

Vibrating systems usually have an infinite number of degrees of freedom (d.o.f.). Since a finite number of measurement d.o.f. can only capture certain deformation patterns, the spatial characteristics of vibrating systems are only partially observed experimentally. This research examines the effects of spatial truncation on non-linear system identification. It is demonstrated that truncation produces frequency correlated noise, which cannot be extracted completely with traditional techniques. The goal of this article is to provide insight and practical recommendations for diagnosing and/or compensating for errors due to spatial truncation in multiple-d.o.f systems. The article demonstrates that non-linear dynamic systems should be instrumented with sufficient sensors; model properties should be used in addition to the input–output data; and additional temporal data should be collected to help diagnose errors due to spatial truncation.

1. INTRODUCTION

Experimental structural dynamic models are restricted in time, frequency, and space. These restrictions are due to practical limitations on the data acquisition or simulation processes. For example, finite sample rates are used to acquire time histories; consequently, the spectral frequency resolution and frequency range of the data is finite as well. The limitation on frequency resolution has long been recognized as a source of bias (leakage) errors [1]. Although the limitations in frequency range and also sensor dynamic range are often overlooked, they are nevertheless a significant source of bias errors. Furthermore, this bias is spatial in nature. The errors actually represent unobserved dynamics of the system in the filtered data. These residual errors in modal or linear vibration data have been well described in the literature [2].

In order to compensate for dynamic residual (bias) errors in linear system identification, modal models of vibrating systems are constructed by estimating and then incorporating the residual dynamics. For instance, researchers have demonstrated that residual information is key to accurately describing the effects of structural modifications on vibrating systems [3–6]. But limitations on the frequency range are not the only source of unobserved dynamics. Residual dynamics also result from the inability to instrument structures with sufficient input/output sensors with infinite dynamic range to fully describe

0022-460X/00/410145 + 17 $35.00/0

all of the modes of vibration. These practical limitations on the number and dynamic range of the input and output measurement degrees of freedom (d.o.f.s) introduces spatial truncation in the modal model. For example, spatial truncation prevents modal analysts from estimating certain modal vectors when transducers are not well placed. Although spatial truncation in linear vibration analysis represents a second order effect, spatial truncation in non-linear vibration analysis is a more serious problem. This paper discusses spatial truncation and its effects on non-linear system identification and parameter estimation.

Many system identification techniques are available for estimating models of non-linear vibrating systems. The literature gives a comprehensive review of each of these techniques [7–12]. All of these techniques depend to some extent on *prior knowledge* of the spatial non-linear structure [13]. Knowledge of the "structure" implies knowledge of the presence, class, and location of all non-linear elements in the system. A spatial approach to non-linear dynamic analysis was introduced in reference [14] and is implemented in references [7, 8, 15, 16] to derive novel characterization and identification techniques for non-linear systems. The fundamental concept in the spatial approach is that structural non-linearities create internal feedback (feedforward) forces, which are functions of the output (input) d.o.f.s. Since spatial resolution of the output d.o.f.s determines the fidelity of non-linear models, the absence of spatial information must be addressed in the context of non-linear system characterization and identification.

Three specific, representative 2-d.o.f. analytical systems are used in the next section to introduce the concept of spatial truncation in non-linear analysis. The results from that section are then extended and generalized to include the effects of spatial truncation on more complicated multiple-degree-of-freedom (m.d.o.f.) non-linear system models. Common examples of truncation in experimental data are described and some conclusions are drawn. The non-linear analysis techniques in references [7, 8] are used as a vehicle for studying the effects of spatial truncation on non-linear system identification.

2. ASPECTS OF SPATIAL TRUNCATION

Three different 2-d.o.f. non-linear systems are shown in Figure 1. Each system has cubic hardening stiffness non-linearities with parameters μ_i in different locations and all the systems have the identical underlying linear structure. A general frequency domain expression which describes all of these systems can be derived using the spatial perspective in reference [7]:

$$\{\mathbf{X}(\omega)\}_{2\times1} = [[\mathbf{H}_L(\omega)]_{2\times2}\ [\mathbf{H}_L(\omega)]_{2\times2}\mu_1(\omega)\ \{\mathbf{B}_{n1}\}_{2\times1} \ldots\ [\mathbf{H}_L(\omega)]_{2\times2}\mu_{N_n}(\omega)\{\mathbf{B}_{nN_n}\}_{2\times1}] \begin{pmatrix} \{\mathbf{F}(\omega)\}_{2\times1} \\ -X_{n1}(\omega) \\ \vdots \\ -X_{nN_n}(\omega) \end{pmatrix}. \tag{1}$$

$[\mathbf{H}_L(\omega)]$ in this system of equations is the frequency response function (FRF) matrix of the underlying (nominal) linear system. $\{\mathbf{F}(\omega)\}$ is the vector of external forces at d.o.f.s 1 and 2. $X_{ni}(\omega)$ is the Fourier transform of the motion across the ith non-linear element. For a cubic hardening stiffness, $X_{ni}(\omega) = \mathbf{F}[(\Delta x_i(t))^3]$, where $\mathbf{F}[\cdot]$ is the Fourier transform operator and $\Delta x_i(t)$ is the relative motion across the ith non-linear stiffness with parameter $\mu_i(\omega)$. The non-linear parameters, $\mu_i(\omega)$, for the static or zero memory non-linear spring in

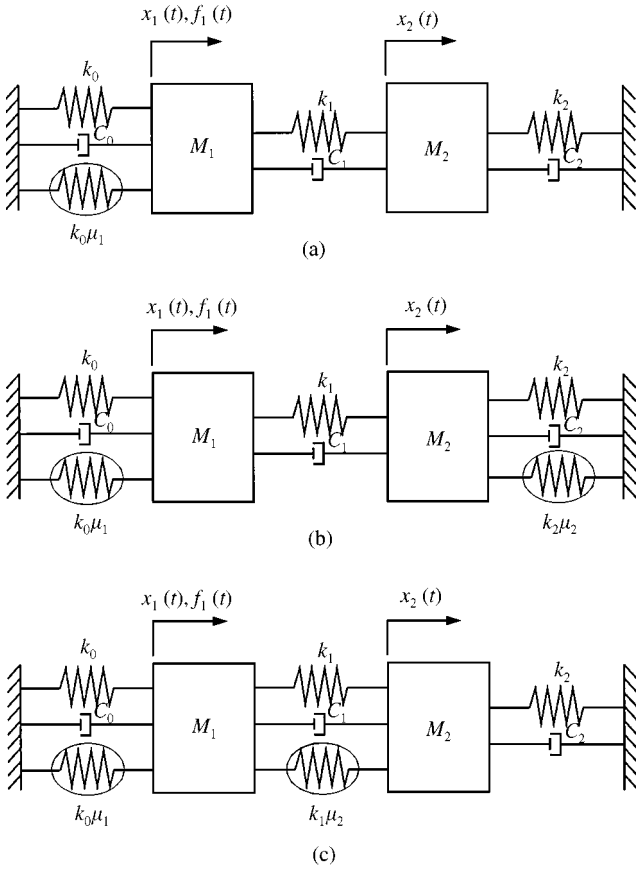

Figure 1. Three-multiple-degree-of-freedom non-linear systems used to illustrate the effects of spatial truncation on non-linear structural dynamic models: (a) System 1 with cubic hardening stiffness to ground at d.o.f. 1, (b) System 2 with cubic hardening stiffnesses to ground at d.o.f.s 1 and 2, (c) System 3 with cubic hardening stiffnesses to ground at d.o.f. 1 and between d.o.f.s 1 and 2.

TABLE 1

Two degree-of-freedom non-linear system parameters

Mass (kg)	Linear damping (N m/s)	Linear stiffness (N/m)	Non-linear parameters ($1/m^2$)
$m_1 = m_2 = 1$	$c_0 = c_1 = c_2 = 2$	$k_0 = k_1 = k_2 = 1000$	$\mu_1 = 500$ $\mu_1 = 500$

Systems 1–3 are constants, μ_i. Lastly, $\{\mathbf{B}_{ni}\}$ is a vector of zeros and ones that determines the location of each of the N_n non-linear elements. This vector is different for each of the systems in Figure 1. The system parameters for the three analytical systems are given in Table 1.

The next three sections examine the effects of spatial truncation on the model in equation (1) for Systems 1–3. The available information for each system consists only of a 30 N root-mean-square, broadband random (normal distribution) applied force at d.o.f. 1, $F_1(\omega) = \mathbf{F}[f_1(t)]$, and the measured response at d.o.f. 1, $X_1(\omega) = \mathbf{F}[x_1(t)]$. Moreover, the

TABLE 2

Simulation parameters for pure random excitation

Δt (s)	Blocksize	Averages	Nyquist frequency (Hz)	Percent overlap
0·00625	4096	150	80	0·70

response at d.o.f. 2 has been truncated from the available simulation data. It is demonstrated how the unobserved dynamics of d.o.f. 2 affect the system identification process differently for the three different systems. The simulation parameters used for all three systems are given in Table 2. A fourth order Runge–Kutta numerical integration scheme was used to simulate the system responses.

2.1. SYSTEM 1

$\{\mathbf{B}_{n1}\}$ for System 1 is equal to $[1\,0]^{\mathrm{T}}$; therefore, the first line of equation (1) for system 1 is given by

$$X_1(\omega) = H_{L11}(\omega)F_1(\omega) - H_{L11}(\omega)\mu_1(\omega)X_{n1}(\omega), \tag{2}$$

$$= [H_{L11} \quad (\omega)\mu_1(\omega)H_{L11}(\omega)]\begin{pmatrix} F_1(\omega) \\ -X_{n1}(\omega) \end{pmatrix}, \tag{3}$$

in which $X_{n1}(\omega) = \mathbf{F}[(x_1(t))^3]$. The FRFs of the underlying linear and non-linear systems are shown in Figure 2. The distortion of the linear system FRF in the direction of higher frequencies is indicative of the non-linear hardening stiffness to ground at d.o.f. 1.

After $X_1(\omega)$, $F_1(\omega)$, and $X_{n1}(\omega)$ are measured or calculated from measured time records, a least-squares solution of equation (3) with spectral averaging is used to simultaneously estimate the FRF of the truncated underlying linear system, $H_{L11}(\omega)$, and the non-linear stiffness parameter, μ_1, from the input and output time data. This identification procedure is called non-linear identification through feedback of the outputs (NIFO) [14]. The ability to *simultaneously* estimate the non-linear parameters and the FRFs of the underlying (nominal) linear system in a single computation is an attractive feature of NIFO. Note that equation (3) indicates there are two forces acting on d.o.f. 1: the external force and the internal feedback force due to the non-linearity. Because the non-linear internal force on d.o.f. 1 is only a function of the observed motion of d.o.f. 1, the NIFO procedure is expected to succeed in this case.

The results of the NIFO procedure for System 1 are shown in Figures 3 and 4. Note that there is near perfect agreement between the estimated and true linear FRFs. The value of $k_0\mu_1$ is also accurately estimated to be $5e5$ N/m^3 from the spectral mean of Figure 4 within 0·5% error. Figure 5 is a plot of the internal force due to the non-linearity. This force characteristic clearly reflects a non-linear, zero memory, cubic stiffness element to ground at d.o.f. 1.

In general, if the unobserved dynamics between the measured and truncated d.o.f.s do not contribute to the internal non-linear feedback, spatial truncation in the data does not affect the parameter estimation process. This is the case for System 1; however, unobserved dynamics create serious errors in the non-linear parameter estimates for Systems 2 and 3.

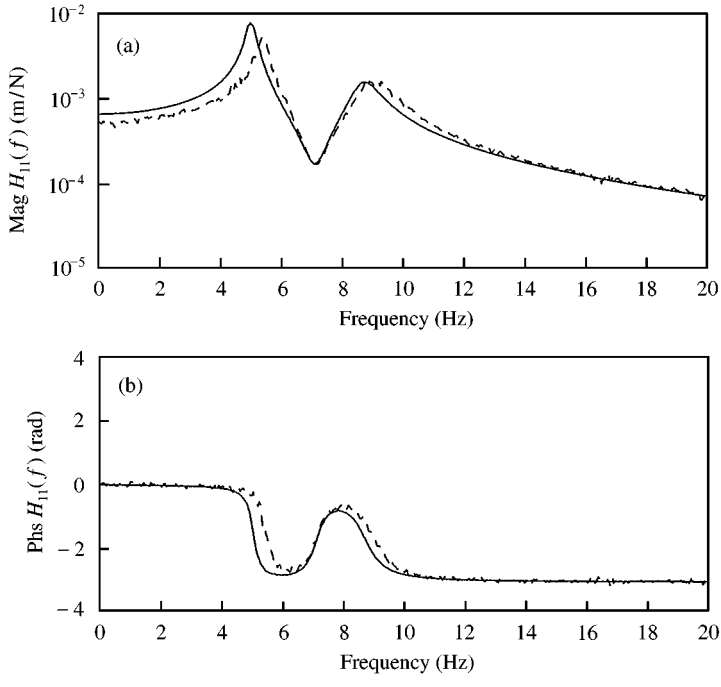

Figure 2. Comparison of the frequency response function of the underlying linear system and the non-linear system of System 1 with a cubic hardening stiffness to ground at d.o.f. 1: ——, linear system; – – –, non-linear system.

2.2. SYSTEM 2

The value of $\{\mathbf{B}_{n1}\}$ for System 2 is the same as for System 1, $[1\ \ 0]^{\mathrm{T}}$. $\{\mathbf{B}_{n2}\}$ for System 2 is equal to $[0\ \ 1]^{\mathrm{T}}$; therefore, the first line of equation (1) for System 2 is given by

$$X_1(\omega) = H_{L11}(\omega)F_1(\omega) - H_{L11}(\omega)\mu_1(\omega)X_{n1}(\omega) - H_{L12}(\omega)\mu_2(\omega)X_{n2}(\omega) \tag{4}$$

$$= [H_{L11}(\omega) \quad \mu_1(\omega)H_{L11}(\omega)]\begin{pmatrix} F_1(\omega) \\ -X_{n1}(\omega) \end{pmatrix} - H_{L12}(\omega)\mu_2(\omega)X_{n2}(\omega) \tag{5}$$

$$= [\mathbf{H}(\omega)\begin{pmatrix} F_1(\omega) \\ -X_{n1}(\omega) \end{pmatrix} - T_2(\omega), \tag{6}$$

where $X_{n2}(\omega) = \mathbf{F}[(x_2(t))^3]$ and $T_2(\omega) \equiv H_{L12}(\omega)\mu_2(\omega)X_{n2}(\omega)$ represent the truncated dynamics. For this system, the motions of both masses determine the internal feedback forces due to the non-linearities; however, the motion of d.o.f. 2 is not observed. This means that the internal force due to the $(x_2(t))^3$ non-linearity cannot be generated from the data in the parameter estimation process. All standard parameter estimation procedures, including NIFO, are expected to fail in this case.

The results of the NIFO procedure for System 2 are shown in Figures 6 and 7. Note the poor quality of the underlying linear FRF estimate near the second mode of vibration. The parameter estimate $\mu_1(\omega)$ is also poor near the second mode of vibration (Figure 7). The goal of this research is to determine why the estimates in $[\mathbf{H}(\omega)]$ are poor, how to diagnose/detect inaccuracies due to truncation, and what to do when there are truncation

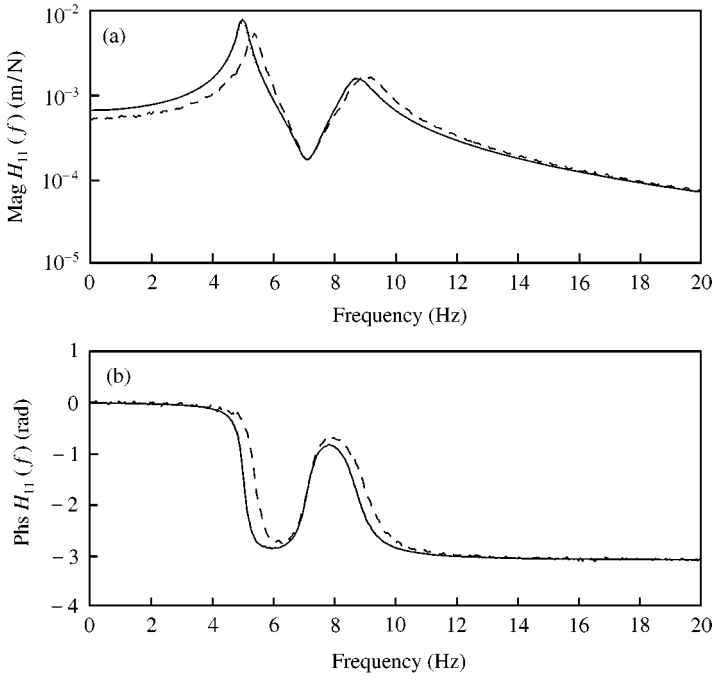

Figure 3. Comparison of the true frequency response function of the underlying linear system, the measured frequency response function of the non-linear system, and the estimated frequency response function of the underlying linear system using NIFO for System 1 with a cubic hardening stiffness to ground at degree of freedom 1: ——, linear system; – – –, non-linear system; ····, linear estimate.

errors in the estimates. The following three points will help in answering these questions: (1) correlated noise due to the truncation is diagnosed using the *unobserved dynamics*; (2) unobserved dynamics in the form of correlated noise are equivalent to *unmeasured internal inputs*; (3) make *all* the right measurements and use data *completely and efficiently*.

According to equation (6), spatial truncation in measured data is a source of correlated noise in the experimental model. The correlated noise consists of everything not extracted from the data. Because there is correlated noise, ordinary least squares does not have the best set of weights to produce unbiased estimates. The first step in diagnosing these errors is to recognize the correlated noise as dynamic, which implies changes as a function of frequency. This is evident in Figure 6, in which the estimate of the underlying linear FRF is accurate through the first mode of vibration, loses accuracy in the antiresonance as the second mode of vibration is reached, and then becomes accurate again beyond the second mode of vibration. Moreover, *the unobserved dynamics provide the means to detect inaccuracies due to truncation.*

The second step is to associate correlated noise with the unmeasured non-linear internal force at the truncated d.o.f. 2. This association helps to explain why the estimate is poor through the antiresonance and near the second mode of vibration. In fact, the non-linear spring to ground at d.o.f. 2 is responsible for the correlated noise and is highly active in this frequency range. Figure 8 gives quantitative proof of this statement. The upper plot is the imaginary part of the $k_0\mu_1(\omega)$ estimate and the lower plot is the FRF between the observed non-linear spectrum X_{n1} and the unobserved non-linear spectrum X_{n2}. When the imaginary part of the parameter estimate reaches a maximum, the error due to spatial

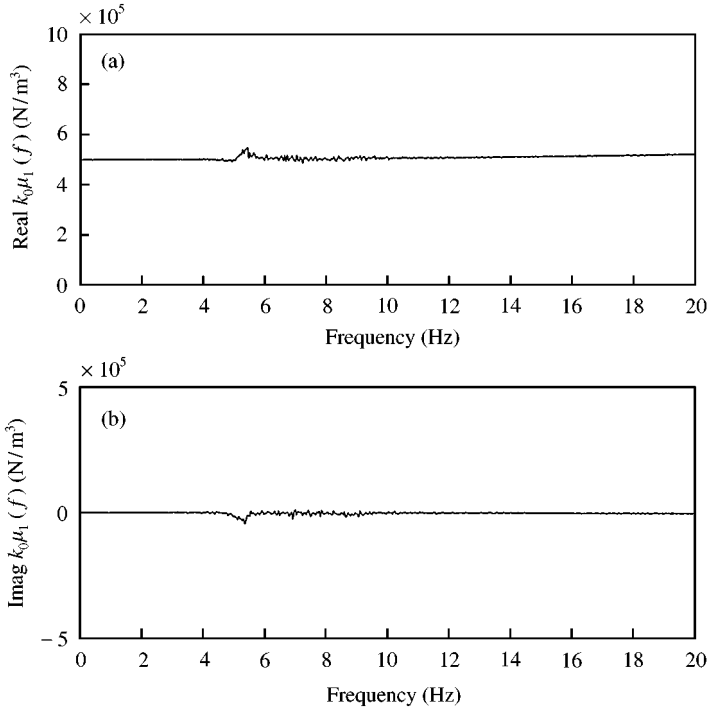

Figure 4. Estimate of the non-linear parameter $k_0\mu_1(\omega)$ in System 1 with a cubic hardening stiffness to ground at degree of freedom 1.

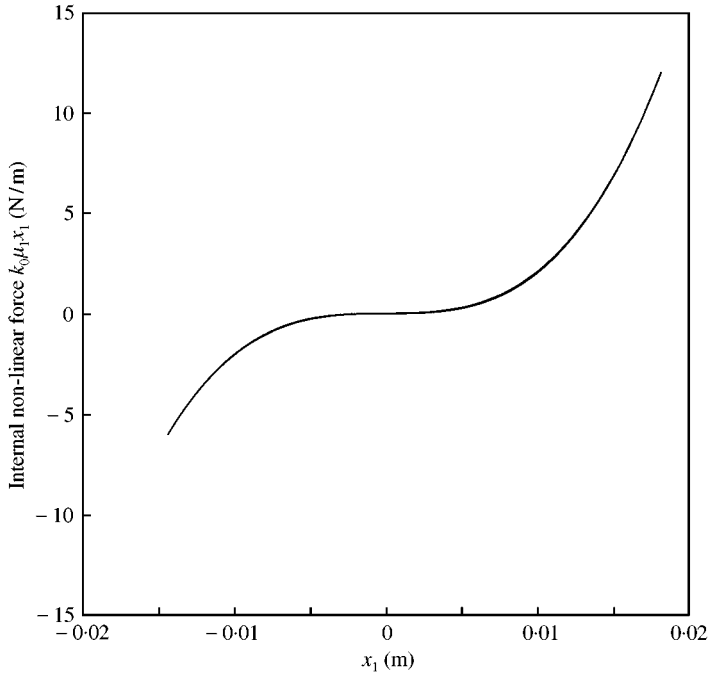

Figure 5. Static (zero memory) characteristic of the non-linear hardening cubic stiffness to ground at d.o.f. 1.

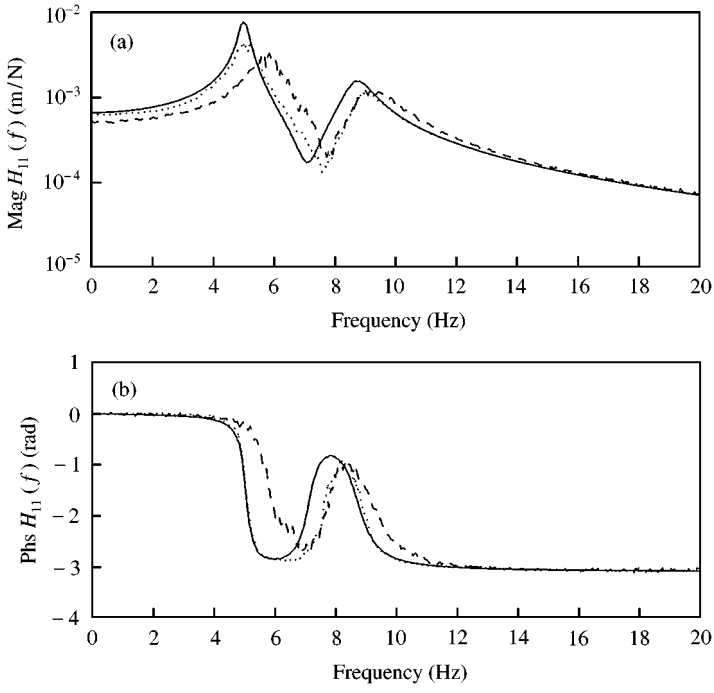

Figure 6. Comparison of the true frequency response function of the underlying linear system, the measured frequency response function of the non-linear system, and the estimated frequency response function of the underlying linear system using NIFO for System 2 with two cubic hardening stiffnesses to ground at d.o.f.s 1 and 2: ——, linear system; – – –, non-linear system; ····, linear estimate.

truncation is a maximum. Note that the frequency where the maximum error occurs matches the frequency where the maximum correlation between the observed $((x_1(t))^3)$ and unobserved $((x_2(t))^3)$ non-linear functions occurs.

The only way to fully diagnose and completely eliminate spatial truncation is to make the right measurements and use all the available data. This is a subtle but important point. For example, consider the parameter estimate in Figure 7. Recall that measured data, $x_1(t), f_1(t)$, and $(x_1(t))^3$, are used in the NIFO procedure to estimate the parameter by making an assumption about the form of the non-linearity, which is a constant parameter cubic spring to ground at d.o.f. 1 (refer to Figure 1). Stated differently there are actually four pieces of data: the three measured or simulated time histories and the assumption about non-linear structure.

Next, compare the assumptions with the estimate in Figure 7. The estimate should be real since the non-linearity is static; however, there is a strong imaginary component near the second mode of vibration, which indicates that non-linear internal forces of some kind enter through $\dot{x}_1(t)$. The unobserved dynamics at d.o.f. 2 flow towards d.o.f. 1 through $\dot{x}_1(t)$. Conversely, the $k_0\mu_1$ parameter estimate is accurate ($\approx 5e5$ N/m^3) where the imaginary component is zero (0–2 and 12–20 Hz).

In addition to the assumption about the non-linear structure, there is another piece of information involving the underlying linear FRF estimate, H_{L11}. According to Hilbert transform theory [17–19], FRFs that describe causal, linear systems have real and imaginary components that are related as follows:

$$\text{Real}\,(H_L(\omega)) = \mathbf{H}[\text{Imag}(H_L(\omega))], \qquad \text{Imag}\,(H_L(\omega)) = -\,\mathbf{H}[\text{Real}\,(H_L(\omega))]. \quad (7, 8)$$

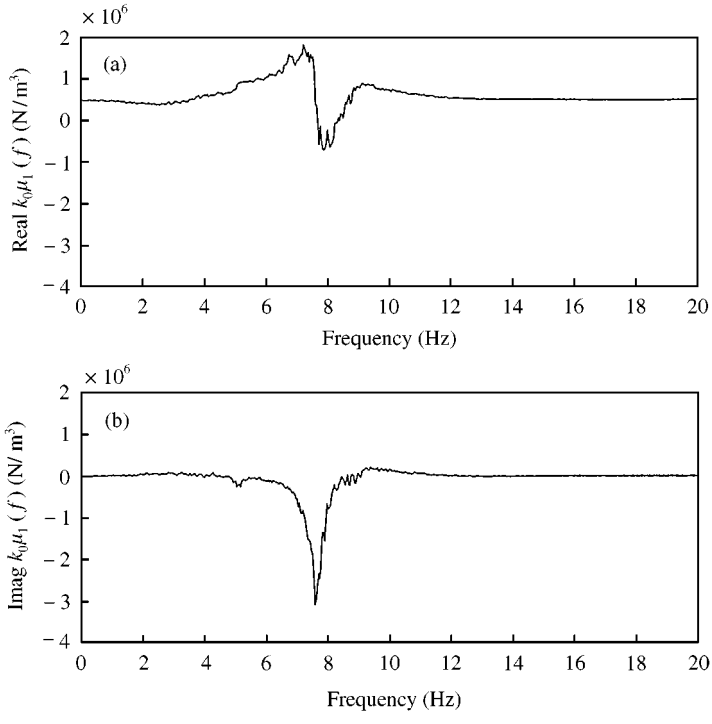

Figure 7. Estimate of the non-linear parameter $k_0\mu_1(\omega)$ in System 2 with two cubic hardening stiffnesses to ground at d.o.f.s 1 and 2 using the truncated data.

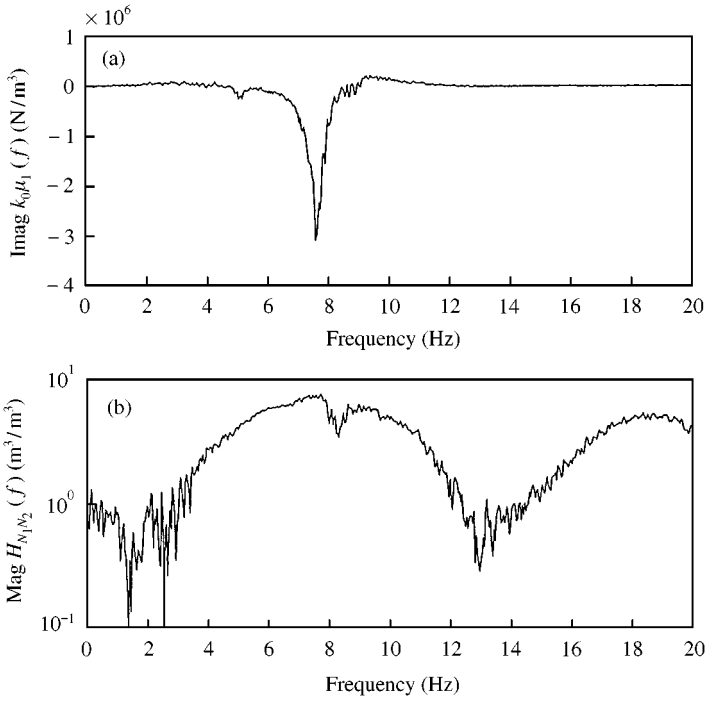

Figure 8. Association between the imaginary error in the non-linear parameter estimate and the frequency response function between the observed non-linear function ($X_{n1}(\omega)$) and the unobserved non-linear function ($X_{n2}(\omega)$) for System 2: (a) Imag$(k_0\mu_1)$; (b) Mag$(H_{N_1N_2})$.

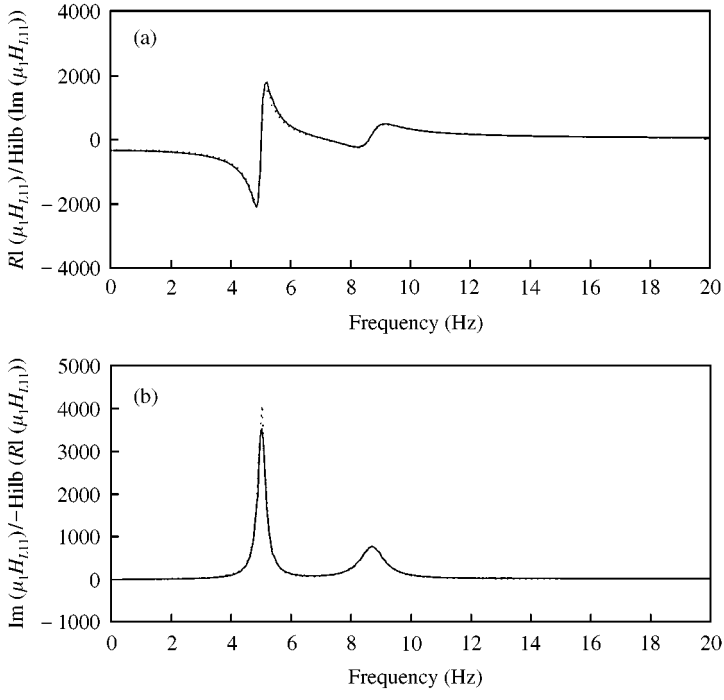

Figure 9. Hilbert transform causality constraint relationships for System 1 parameter estimate, $k_0\mu_1 H_{L11}(\omega)$: (a) Real$(k_0\mu_1 H_{L11})$, solid curve (——), $\mathbf{H}$[Imag$(k_0\mu_1 H_{L11})$], dashed curve (- - -); (b) Imag$(k_0\mu_1 H_{L11})$, solid curve (——), $\mathbf{H}[-\text{Real}(k_0\mu_1 H_{L11})]$, dashed curve (- - -).

Equations (7) and (8), constitute an additional piece of information which can help diagnose spatial truncation errors. If the FRF parameter estimate does not satisfy these equations, there may be truncation errors in the estimate(s). For instance, the Hilbert transform causality constraint plots for the linear FRF estimates of System 1 are shown in Figure 9. Note that the real and imaginary parts of the estimate in the system without truncation form a Hilbert transform pair. In contrast, the Hilbert transform causality constraint plots for the linear FRF estimates of System 2 are shown in Figure 10. The causality constraints for these estimates are violated because of the unobserved dynamics at d.o.f. 2; therefore, the estimates are incorrect. This is evident in the distortion near the first mode of vibration in the lower plot of Figure 10.

2.3. SYSTEM 3

The value of $\{\mathbf{B}_{n1}\}$ for System 3 is the same as for System 1, $[1\ \ 0]^{\mathrm{T}}$. $\{\mathbf{B}_{n3}\}$ for System 3 is equal to $[1\ \ -1]^{\mathrm{T}}$; therefore, the first line of equation (1) for System 3 is given by

$$\begin{aligned} X_1(\omega) &= H_{L11}(\omega)F_1(\omega) - H_{L11}(\omega)\mu_1(\omega)X_{n1}(\omega) \\ &\quad - (H_{L11}(\omega) - H_{L12}(\omega))\mu_2(\omega)X_{n2}(\omega) \\ &= [H_{L11}(\omega) \quad \mu_1(\omega)H_{L11}(\omega)] \begin{pmatrix} F_1(\omega) \\ -X_{n1}(\omega) \end{pmatrix} \end{aligned} \tag{9}$$

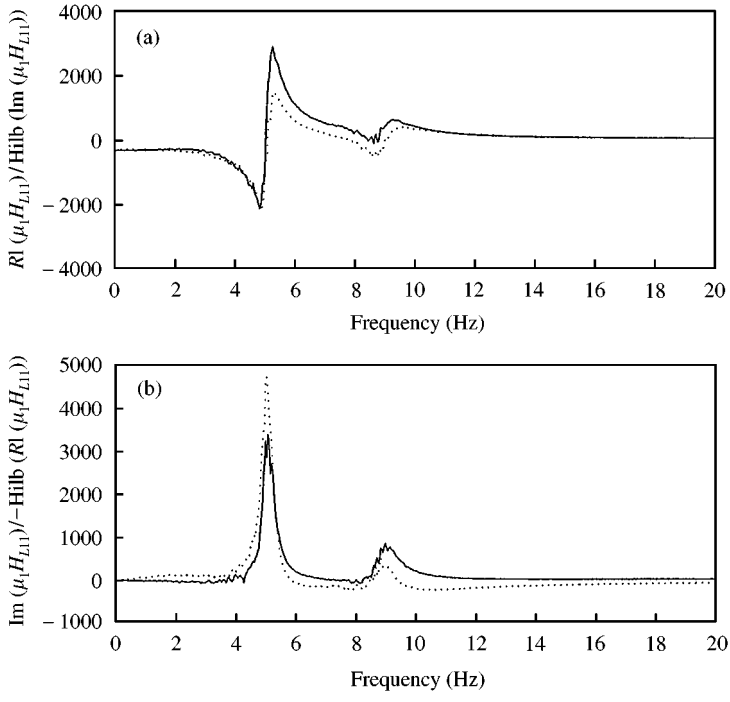

Figure 10. Hilbert transform causality constraint relationships for System 2 parameter estimate, $k_0\mu_1 H_{L11}(\omega)$: (a) Real$(k_0\mu_1 H_{L11})$, solid curve (——), $\mathbf{H}$[Imag$(k_0\mu_1 H_{L11})$], dashed curve (- - -); (b) Imag$(k_0\mu_1 H_{L11})$, solid curve (——), $\mathbf{H}$[− Real$(k_0\mu_1 H_{L11})$], dashed curve (- - -).

$$- (H_{L11}(\omega) - H_{L12}(\omega))\,\mu_2(\omega)\,X_{n2}(\omega) \tag{10}$$

$$= [\mathbf{H}(\omega)] \begin{pmatrix} F_1(\omega) \\ -X_{n1}(\omega) \end{pmatrix} - T_3(\omega), \tag{11}$$

where $X_{n2}(\omega) = \mathbf{F}[(x_1(t) - x_2(t))^3]$ and $T_3(\omega) \equiv (H_{L11}(\omega) - H_{L12}(\omega))\,\mu_2(\omega)\,X_{n2}(\omega)$. Equation (11) for System 3 is very similar to equation (6) for System 2 except the correlated noise due to truncation is different in each system. The NIFO procedure is also expected to fail for System 3.

The results of the NIFO procedure for System 3 are shown in Figures 11 and 12. Note the similarities with the results for System 2 in Figures 6 and 7. The most significant difference is in the accuracy (i.e., smaller imaginary part) of the non-linear parameter estimate for System 3 when compared to the estimate for System 2 (refer to Figures 7 and 12). In fact, the estimate is approximately equal to $5e5$ N/m^3 from 0 to 6 Hz and 0 to 20 Hz, and the error is less severe near the second mode of vibration than for System 2.

Figure 13 shows the FRF between the observed and unobserved non-linear functions for System 3. The parameter estimate for System 3 is more accurate than for System 2 because the correlation between the observed non-linear spectrum, $X_{n1}(\omega)$, and the unobserved non-linear spectrum, $X_{n2}(\omega)$, is less for System 3 than for System 2 (cf. compare Figure 13 with Figure 8). These results are generalized in the next section.

2.4. GENERAL SYSTEM

For general m.d.o.f. non-linear vibrating systems, system identification and parameter estimation are always subject to spatial truncation. Common examples of spatial truncation

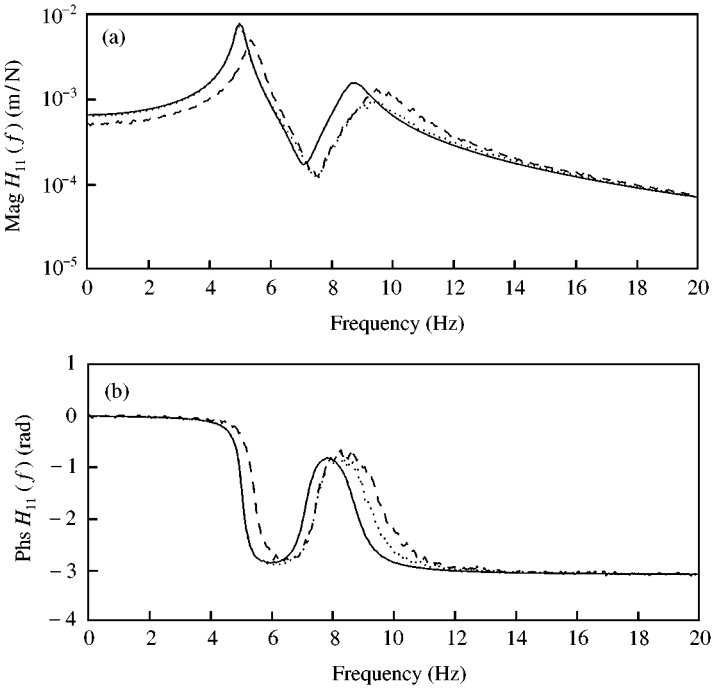

Figure 11. Comparison of the true frequency response function of the underlying linear system, the measured frequency response function of the non-linear system, and the estimated frequency response function of the underlying linear system using NIFO for System 3 with a cubic hardening stiffness to ground at d.o.f. 1 and a cubic hardening stiffness between d.o.f.s 1 and 2: ——, linear system; - - -, non-linear system; ····, linear estimate.

include:

- Dynamics between observed d.o.f. and the d.o.f. to which non-linearities are attached (e.g., Systems 2 and 3 above).
- Unmeasured dynamics at d.o.f.s along multiple axes (e.g., uniaxial accelerometers are used instead of triaxial accelerometers).
- Unmeasured dynamics at rotational d.o.f.s (e.g., rotational motions across engine mounts are not measured).
- Unmeasured or unused portions of the state (e.g., non-linear function of the position is used instead of the actual non-linear function of the velocity).
- Unmeasured or unknown initial conditions on the states.
- Unmeasured motions beyond the dynamic range of sensors.

Spatial truncation in vibration data can produce poor estimates of non-linear parameters and underlying linear FRFs. When the NIFO procedure or any other frequency domain identification technique is used, truncation can be diagnosed by considering the following points:

1. The non-linear parameters $\mu_1(\omega)$ should be *real* when the non-linear elements are assumed to have parameters of a specific form.
2. The real and imaginary parts of all nominal/underlying linear $H_{Lpq}(\omega)$ FRF estimates should satisfy the Hilbert transform causality constraints (equations (7) and (8)).
3. The estimates of the nominal/underlying linear FRFs $H_{Lpq}(\omega)$ and $H_{Lqp}(\omega)$ should be equal (*reciprocity*).

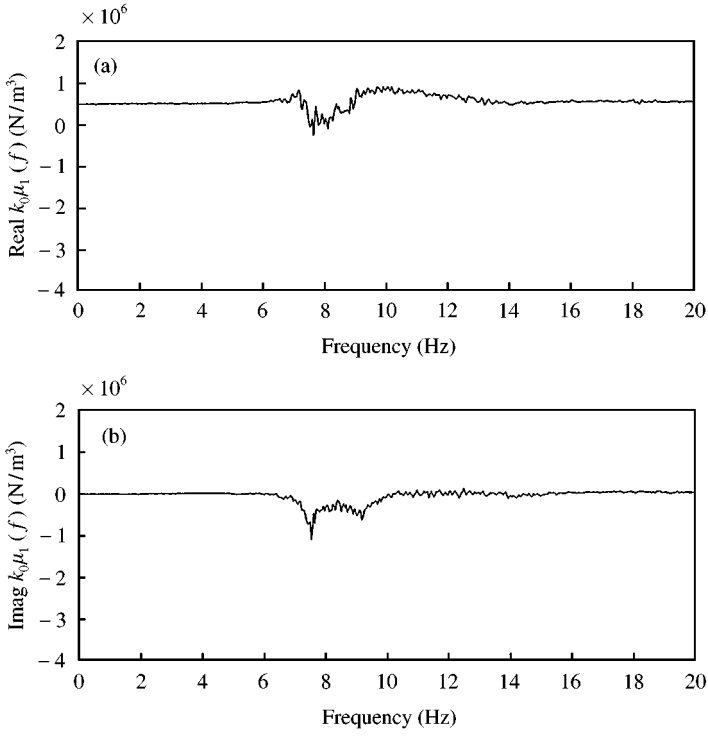

Figure 12. Estimate of the non-linear parameter $k_0\mu_1(\omega)$ in System 3 with a cubic hardening stiffness to ground at d.o.f. 1 and a cubic hardening stiffness between d.o.f.s 1 and 2 using the truncated data.

4. The estimates of the nominal/underlying linear FRFs $H_{Lpq}(\omega)$ should be approximately equal to a measured set of FRFs around the nominal operating point of interest.
5. Partial and ordinary coherence functions should account for all of the energy in the output due to the external forces and the internal non-linear feedback forces that can be observed [9].
6. The nominal/underlying linear FRF estimates and the non-linear parameter estimates should be invariant for different excitation levels.
7. The autocorrelation function of the residual in the frequency domain estimate should be an impulse function (i.e., the residual should be white noise that is uncorrelated with the input).

By implementing these ideas, fairly accurate parameters for complicated m.d.o.f. non-linear systems with multiple non-linearities can be estimated as in reference [8]. These seven evaluation criteria are in keeping with the tenet of experimental dynamics mentioned earlier: make all the right measurements and use data efficiently and completely. For example, the fourth and sixth points in the list above suggest that additional temporal data can help to diagnose and partially compensate for spatial truncation. In particular, measured system FRFs for relatively small input levels around the nominal operating point help to characterize truncated dynamics, whereas input–output data sets for various input levels can be used to actually model the truncated dynamics. These ideas are demonstrated next for System 3.

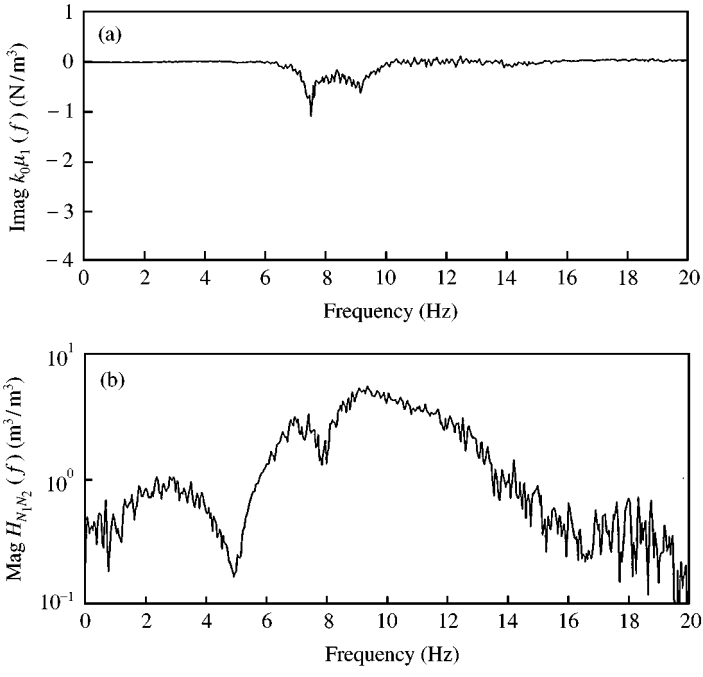

Figure 13. Association between the imaginary error in the non-linear parameter estimate and the frequency response function between the observed non-linear function ($X_{n1}(\omega)$) and the unobserved non-linear function ($X_{n2}(\omega)$) for System 3: (a) Imag$(k_0\mu_1(\omega))$; (b) Mag$(H_{N_1N_2}(\omega))$.

2.5. PARTIAL COMPENSATION

Although spatial truncation errors can be diagnosed using techniques described in the previous section, the errors cannot be completely eliminated. Moreover, it is generally not practical to recover from a poorly planned experimental dynamic test. When the d.o.f.s are not chosen correctly in a complicated system (e.g., automobile suspension and chasis), there may be extreme truncation and numerous sources of correlated noise. This makes it practically impossible to estimate accurate parameters. It is recommended to instrument systems of this type with sufficient sensors and actuators to prevent spatial truncation.

Partial compensation of the correlated errors due to spatial truncation can be achieved in some instances. In particular, when non-linear internal forces are uncorrelated over certain frequency ranges, the parameter estimates within these ranges are fairly accurate and can be used to iterate using the constraints discussed in the previous section. For instance, the spectral mean of the estimate in Figure 12 over the low- and high-frequency ranges matches the true parameter value.

It may also be possible in many instances to use the parameter estimates in Figure 1 to predict dynamic behaviour. For example, even though estimates of the real and imaginary parts of the non-linear parameter estimate for System 3 are inaccurate, the parameters do accurately describe the vibration response for the *given input type and amplitude*. Moreover, if the input types and levels are similar in a different vibration test, the parameter estimates can be used along with measured data to predict the actual response of the system.

Multiple temporal data sets can also be taken to help characterize and identify the truncation dynamics. For example, Figure 14 shows the surface which is generated by exciting System 3 with 1, 2, 4, 8, 16, and 32 N broadband random inputs and then

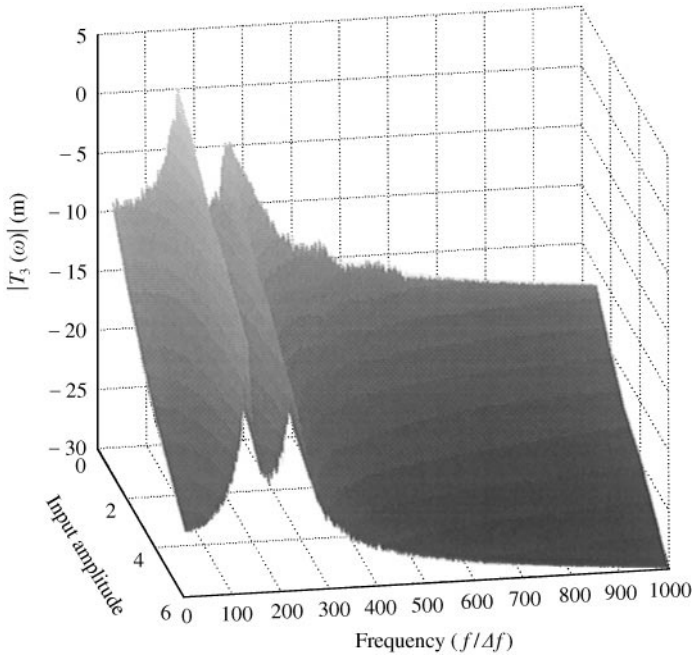

Figure 14. Truncation surface for System 3 estimated for six different excitation levels.

approximating the truncation dynamics from equation (11):

$$-T_3(\omega) \approx X_1(\omega) - \hat{H}_{L11}(\omega)F_1(\omega) - \hat{H}_{L11}(\omega)\mu_1(\omega)X_{n1}(\omega). \tag{12}$$

$\hat{H}_{L11}(\omega)$ in this expression is the measured estimate of the underlying linear FRF for small input levels around the nominal point and $\hat{\mu}_1(\omega)$ is the estimate of the non-linear parameter for the spring to ground at d.o.f. 1. Recall from Figure 12 that the estimate at low and high frequencies is approximately equal to the true value, $5e5\,\mathrm{N/m^3}$. When taken together, the underlying linear FRF, $\hat{H}_{L11}(\omega)$, non-linear parameter, $\hat{\mu}_1(\omega)$, and the *truncation surface* in Figure 14 form a complete non-linear impedance model of System 3 over the input range from 1 to 32 N. This technique for identifying a forced response impedance model of a system in spite of spatial measurement truncation is similar to the restoring force approach by Masri *et al.* [11].

3. SUMMARY AND CONCLUSIONS

Spatial truncation in experimental models of vibrating systems has been explored and insight has been given for diagnosing correlated errors associated with truncation. These errors can be diagnosed and sometimes eliminated by utilizing input–output data in addition to information about the assumed model including: the form of the non-linear parameter estimates; Hilbert transform causality constraints and reciprocity constraints on the estimates of the underlying linear FRFs; additional temporal data for different excitation levels (truncation surfaces); and the correlation of the residuals in the frequency domain estimates. The main conclusion is that non-linear vibrating systems should be

instrumented with sufficient sensors to avoid truncation and to estimate accurate parameters.

REFERENCES

1. J. S. BENDAT and A. G. PIERSOL 1986. *Random Data*: *Analysis and Measurement Procedures*. New York: John Wiley & Sons.
2. D. J. EWINS 1984 *Modal Testing*: *Theory and Practice*. Somerset, England: Research Studies Press Ltd.
3. P. AVITABILE, J. O'CALLAHAN and F. PECHINSKY 1990 *Proceedings of the International Modal Analysis Conference*, Vol. I, 43–54. Understanding structural dynamic modification truncation.
4. R. C. SOHANEY and D. BONNECASE 1989 *Proceedings of the International Modal Analysis Conference*, Vol. I, 568–574. Residual mobilities and structural dynamic modifications.
5. N. OKUBO and T. MATSUZAKI 1989 *Proceedings of the International Modal Analysis Conference*, Vol. I, 578–583. Determination of residual flexbility and its effective use in structural modification.
6. A. GIRARD and J. F. IMBERT 1987 *Proceedings of the International Modal Analysis Conference*, Vol. I, 820–826. Modal effective parameters and truncation effects in structural dynamics.
7. D. E. ADAMS and R. J. ALLEMANG 1999 *Mechanical Systems and Signal Processing*. A frequency domain method for estimating the parameters of a nonlinear structural dynamic model through feedback (accepted for publication).
8. D. E. ADAMS and R. J. ALLEMANG 2000 *Proceedings of the International Modal Analysis Conference*, Vol. I, 725–732. New spatial MDOF characterization and identification techniques for nonlinear systems.
9. J. S. BENDAT 1998 *Nonlinear Systems Techniques and Applications*. New York: John Wiley & Sons.
10. C. M. RICHARDS and R. SINGH 1998 *Journal of Sound and Vibration* **213**, 673–708. Identification of multi-degree-of-freedom non-linear systems under random excitations by the "reverse path" spectral method.
11. S. F. MASRI, H. SASSI and T. K. CAUGHEY 1982 *Journal of Applied Mechanics* **49**, 619–627. Nonparametric identification of nearly arbitrary nonlinear systems.
12. D. E. ADAMS and R. J. ALLEMANG 1999 *Proceedings of the International Modal Analysis Conference XVII*, Vol. I, 315–322. Demonstration of multiple degree of freedom nonlinear system identification using time and frequency domain methods.
13. C. M. RICHARDS and R. SINGH 1998 *Journal of Sound and Vibration* **220**, 413–450. Feasibility of identifying non-linear vibratory systems consisting of unknown polynomial forms.
14. D. E. ADAMS and R. J. ALLEMANG 1999 *Journal of Sound and Vibration* **227**, 1083–1108. A new derivation of the frequency response function matrix for vibrating nonlinear systems.
15. D. E. ADAMS and R. J. ALLEMANG 1999 *Proceedings of the International Modal Analysis Conference XVII*, Vol. **I**, 1195–1202. A spatial method of characterizing nonlinearities in multiple degree of freedom vibrating systems.
16. D. E. ADAMS and R. J. ALLEMANG 1999 *Journal of Vibration and Acoustics* **121**, 495–500. Characterization of nonlinear vibrating systems using internal feedback and frequency response modulation.
17. N. THRANE 1984 *Hewlett Packard Application Notes*. The Hilbert transform.
18. M. SIMON and G. R. TOMLINSON 1984 *Journal of Sound and Vibration* **96**, 421–436. Use of the Hilbert transform in modal analysis of linear and non-linear structures.
19. K. WORDEN and C. R. TOMLINSON 1990 *Proceedings of the International Modal Analysis Conference* Vol. 1, 121–130. The high-frequency behaviour of frequency response functions and its effect on their Hilbert transforms.
20. A. E. BRYSON Jr and YU-CHI HO 1975 *Applied Optimal Control*: *Optimization*, *Estimation*, *and Control*. New York: Hemisphere Publishing Corporation.

APPENDIX A: NOMENCLATURE

d.o.f.(s)	degree(s) of freedom
s.d.o.f.	single degree of freedom
m.d.o.f.	multiple degrees of freedom

NIFO	nonlinear identification through feedback of the outputs
N_o	number of output (response) degrees of freedom
N_i	number of input (forced) degrees of freedom at which the input is non-zero; there are N_o total input degrees of freedom
N_n	number of non-linear elements in the model
FRF(s)	frequency response function(s)
$\{\mathbf{x(t)}\}_{N_o \times 1}$	measured output time history vector of length N_o
$\{\mathbf{f(t)}\}_{N_o \times 1}$	measured input time history vector of length N_o
$\{\mathbf{X}(\omega)\}_{N_o \times 1}$	linear Fourier spectrum of the output vector
$\{\mathbf{F}(\omega)\}_{N_o \times 1}$	linear Fourier spectrum of the input vector
$[\mathbf{H}_L(\omega)]_{N_o \times N_o}$	frequency response function matrix of a linear or linearized system
$H_{Lpq}(\omega)$	frequency response function between input d.o.f. q and output d.o.f. p for underlying linear system
$H_{pq}(\omega)$	frequency response function between input d.o.f. q and output d.o.f. p
$\mu_i(\omega)$	scalar non-linear parameter for non-linear element i
$X_{ni}(\omega)$	scalar non-linear function of the outputs for non-linear element i
$\{\mathbf{B}_{ni}\}_{N_o \times 1}$	vector of impedance with non-linear coefficient factored out to yield entries of 1 and -1 only; associated with non-linear element i
$\mathbf{F}[\cdot]$	Fourier transform operator
$\mathbf{H}[\cdot]$	Hilbert transform operator